Catalysis Today 149 (2010) 401–406

Contents lists available at ScienceDirect

Catalysis Today

journal homepage: www.elsevier.com/locate/cattod

The effect of the addition of Y_2O_3 to Ni/α-Al_2O_3 catalysts on the autothermal reforming of methane

Danielle C.R.M. Santos, Laureanny Madeira, Fabio B. Passos *

Departamento de Engenharia Química e Petróleo, Universidade Federal Fluminense (UFF), Rua Passo da Pátria, 156, 24210-240 Niterói, RJ, Brazil

ARTICLE INFO

Article history:
Available online 22 July 2009

Keywords:
Autothermal reforming
Nickel catalysts
Yttria
Methane conversion

ABSTRACT

The addition of Y_2O_3 to Ni/α-Al_2O_3 catalysts was investigated by BET surface area measurements, hydrogen chemisorption, X-ray diffraction, UV–vis diffuse reflectance spectroscopy, X-ray fluorescence, temperature programmed reduction, temperature programmed oxidation and cyclohexane dehydrogenation. Autothermal reforming experiments were performed in order to evaluate the methane conversion and proceeded through an indirect mechanism consisting of total combustion of methane followed by CO_2 and steam reforming generating the synthesis gas. The Y_2O_3·Al_2O_3 supported catalysts presented better activity and stability in autothermal reforming reaction. Temperature programmed oxidation analysis demonstrated that the addition of Y_2O_3 resulted in a change of the type or the location of coke formed during reaction. None of the prepared catalyst presented deactivation by sintering under the tested conditions. The improved stability of supported catalysts Y_2O_3·Al_2O_3 was the result of minimizing the formation of coke on the surface of nickel particles.

1. Introduction

Autothermal reforming of methane is considered the best choice for producing synthesis gas for large scale GTL (gas-to-liquids) plants [1–3]. In this process, partial oxidation of methane and steam reforming of methane are combined in the same reactor. There is an optimization of energy consumption since partial oxidation occurs in a burner after mixing of the feedstock and provides energy for the downstream endothermic reforming reactions [4,5]. The economics of this process is favored by an improved design of reactor, burner and heat exchangers. Besides, the H_2/CO ratio can be adjusted varying the $CH_4/O_2/H_2O$ composition in the feedstock, resulting in a H_2/CO ratio close to 2, the desired composition of synthesis gas for Fischer–Tropsch synthesis. Additionally, in order to avoid the need for CO_2 recycling low H_2O/CH_4 ratios must be used [1,2].

The autothermal reforming of methane can be catalyzed by several transition metals, with Pt, Rh and Ru being the most catalytic active. However, Ni has been used due to its low cost and availability [6]. However, carbon deposition due to the severe operational conditions of the reactor also affects the catalytic behavior. In order to extend the lifetime and stability of nickel catalysts, promoters are added, which act as support or active phase modifiers, decreasing the carbon deposition and consequently improving the stability of the catalysts [7,8].

Y_2O_3 has been used as a support for metal catalysts used in methane conversion [8] and improved results have been obtained in terms of stability of the catalysts. In this paper, the addition of Y_2O_3 to Ni/α-Al_2O_3 catalyst was investigated by BET surface area determination, hydrogen chemisorption, X-ray diffraction (XRD), UV–vis diffuse reflectance spectroscopy (DRS), temperature programmed reduction (TPR), temperature programmed oxidation (TPO) and cyclohexane dehydrogenation. Autothermal reforming experiments under low H_2O/CH_4 ratios were performed in order to evaluate the methane conversion and the stability of the catalysts.

2. Experimental

2.1. Catalyst preparation

All nickel catalysts were prepared by incipient wetness impregnation of a $Ni(NO_3)_2$·$6H_2O$ solution with successive impregnation and intermediate drying. After impregnation, the samples were dried at 120 °C for 12 h and calcined (10 °C/min) in a muffle at 650 °C for 6 h (10 °C/min). α-Al_2O_3 (ALCOA 1.5 m^2/g) was used as support after calcination at 800 °C for 6 h. Y_2O_3 support was prepared by calcination of $Y(NO_3)_3$·$6H_2O$ at 800 °C for 1 h. Y_2O_3·α-Al_2O_3 supports, with different yttria contents, were prepared by impregnation of α-Al_2O_3 with an $Y(NO_3)_3$·$6H_2O$ solution, following by drying at 120 °C and calcination at 800 °C for 6 h.

* Corresponding author. Tel.: +55 21 2629 5599.
E-mail address: fbpassos@vm.uff.br (F.B. Passos).

0920-5861/$ – see front matter © 2009 Elsevier B.V. All rights reserved.
doi:10.1016/j.cattod.2009.06.015

2.2. BET surface area

Surface area measurements were performed in a Micromeritics ASAP 2010 device. About 1.5 g of each sample was introduced in a quartz cell and attached to the adsorption apparatus. The sample was dried under vacuum at 220 °C for 10 h. The BET surface area was obtained by N_2 adsorption at 77 K.

2.3. X-ray diffraction (XRD)

X-ray diffraction measurements were carried out using a Rigaku (Miniflex) diffractometer with a Cu Kα radiation. The XRD data of calcined samples were collected at 0.04°/step with integration times of 1 s/step and a 2θ range of 2–90°.

2.4. UV–vis diffuse reflectance spectroscopy (DRS)

The samples were characterized at room temperature using a Cary 500 (Varian) spectrophotometer equipment. In order to separate the contribution of the support, the reflectance $R(\alpha)$ of the sample was made proportional to the reflectance of Al_2O_3, and the "Kubelka–Munk" function $F(R)$ was calculated.

2.5. Temperature programmed reduction (TPR)

Temperature programmed reduction (TPR) experiments were performed in a quartz micro-reactor coupled to a quadrupole mass spectrometer (Balzers, Omnistar). The samples (150 mg) were dehydrated at 150 °C for 30 min in a He flow prior to reduction. After cooling to room temperature, a mixture of 5%H_2 in Ar flowed through the sample at 30 mL/min, and the temperature was raised at a heating rate of 10 °C/min up to 1000 °C.

2.6. Hydrogen chemisorption

Hydrogen chemisorption was performed by a volumetric method in a Micromeritcs ASAP 2010C device. The sample (500 mg) pretreatment consisted of drying at 150 °C for 30 min under a 30 mL/min He flow, followed by reduction under 30 mL/min of H_2 at 800 °C. The samples were outgassed under vacuum of 500 °C. All the chemisorption measurements were performed at 35 °C. Both total and reversible H_2 isotherms were measured. H/Ni ratios were calculated using the irreversible H_2 uptake.

2.7. Cyclohexane dehydrogenation

Cyclohexane conversion was used as a structure-insensitive reaction to evaluate the number of exposed Ni atoms of the samples. This reaction was performed at atmospheric pressure in a flow quartz reactor (13 mm i.d.). The samples (100 mg) were previously dried at 150 °C for 30 min under He flow (30 mL/min) and reduced at 800 °C under H_2 flow (30 mL/min). The reactant mixture was obtained by bubbling hydrogen through a saturator containing cyclohexane at 12 °C (H_2/C_6H_{12} = 13.6). The temperature was varied between 250 and 320 °C. The effluent gas phase was analyzed by an on-line gas chromatograph (HP-5890) equipped with a flame ionization detector and an HP Innowax capillary column. Under these conditions, there was no significant deactivation of the catalysts and there were no diffusional or thermodynamic limitations.

2.8. Autothermal reforming of methane

Autothermal reforming of methane was performed in a continuous quartz reactor (13 mm i.d.) at atmospheric pressure. The samples were previously dried at 150 °C for 30 min under He flow (30 mL/min) and reduced at 800 °C under H_2 flow (30 mL/min) for 2 h. The reaction was carried out at 800 °C. A reactant mixture containing (67 mL/min), O_2 (33 mL/min) and H_2O (12.6 mL/min) was used. The H_2O content of the feed stream was obtained by flowing the CH_4 and O_2 reactant mixture through a saturator containing H_2O at 49 °C. CH_4:O_2 ratio of 2:1 and a flow rate of 100 mL/min were used. In order to avoid temperature gradients, the catalyst samples (10 mg) were diluted with inert SiC (90 mg). The exit gases were analyzed using a gas chromatograph VARIAN CP3800 equipped with a thermal conductivity detector (TCD) and a Supelco Carboxen 1010 tplot column.

2.9. Temperature programmed oxidation (TPO)

TPO experiments were performed in a multipurpose unit coupled to a Balzers Omnistar quadrupole mass spectrometer. The samples, used previously in the autothermal reforming reaction, were dried at 150 °C for 30 min, under He flow (30 mL/min) and cooled to room temperature, followed by an increase of temperature under O_2/He (30 mL/min) flow in a rate of 10 °C/min to 800 °C.

2.10. Catalyst ageing experiments

The samples (100 mg) were previously dried at 150 °C for 30 min, under He flow (30 mL/min) and reduced at 800 °C under H_2 flow (30 mL/min). The catalysts were aged at 800 °C during 24 h over all catalysts under a gas mixture containing He (30 mL/min) and H_2O (3.8 mL/min) obtained using a saturator at 49 °C. The samples were transferred to the cyclohexane conversion reaction system in order to evaluate the number of surface metallic sites after the ageing processes. The samples were dried at 150 °C for 30 min under He flow (30 mL/min) and reduced at 500 °C under H_2 flow (30 mL/min), before the activity was tested under the same conditions already described for the conversion of cyclohexane.

3. Results and discussion

3.1. BET surface area

The surface areas of the prepared catalysts are shown in Table 1. The 8%Ni/α-Al_2O_3 catalyst showed a surface area equal to 3.7 m^2/g, consistent with the fact that α-Al_2O_3 was used as support [9,10]. The Ni/Y_2O_3 catalyst showed a BET surface area of 18.6 m^2/g which is higher than the typical value of 10 m^2/g reported in the literature for Y_2O_3 supported catalysts [11–14], probably due to the differences in the preparation method used for Y_2O_3. The Y_2O_3·Al_2O_3 supported catalysts showed an increase in the surface area with the increase of Y_2O_3 content.

3.2. X-ray diffraction (XRD)

Fig. 1 presents the diffractograms of α-Al_2O_3, Y_2O_3 and Y_2O_3·Al_2O_3 and of the respective nickel supported catalysts. The vertical dotted lines indicate NiO diffraction peak positions. In the case of the 8%Ni/α-Al_2O_3 the diffraction pattern included NiO lines

Table 1
BET surface area of Ni/α-Al_2O_3, Ni/Y_2O_3·Al_2O_3 and Ni/Y_2O_3 catalysts.

Catalyst	BET surface area (m^2/g)
8%Ni/α-Al_2O_3	3.7
8%Ni/Y_2O_3	18.6
8%Ni/2%Y_2O_3·Al_2O_3	5.8
8%Ni/2.5%Y_2O_3·Al_2O_3	6.4
8%Ni/5%Y_2O_3·Al_2O_3	8.2

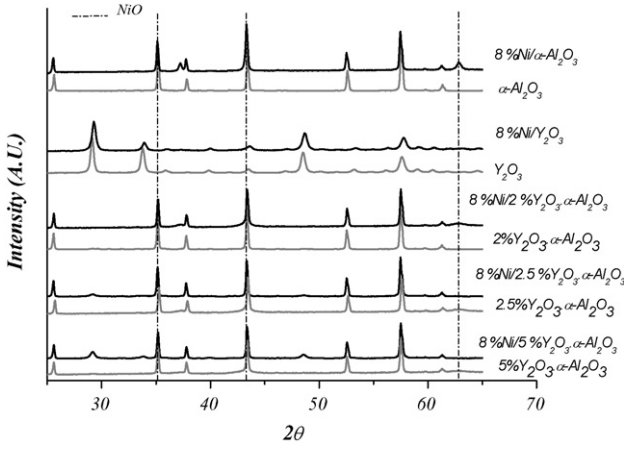

Fig. 1. XRD of α-Al_2O_3, Y_2O_3,Y_2O_3·Al_2O_3 and respective nickel supported catalysts.

and a typical α-Al_2O_3 diffractogram, as previously observed in the literature [9,15]. NiO diffraction lines were not observed in the case of the 8%Ni/Y_2O_3, this might be related to a better Ni dispersion on this support [9,16], and additionally to a formation of a surface compound between Ni and Y_2O_3, as also indicated by the TPR results. For catalysts containing 20%Ni/Y_2O_3 [17], NiO diffraction lines were observed, but for 3%Ni/Y_2O_3 [9], NiO diffraction lines were not observed, indicating that lower Ni contents can be better dispersed on the Y_2O_3 support. The XRD patterns of Y_2O_3·Al_2O_3 were a simple superposition of Y_2O_3 and α-Al_2O_3 diffraction patterns indicating there was no formation of a solid solution between the two oxides. NiO diffraction lines were not observed for all Ni/Y_2O_3·Al_2O_3 catalyst XRD patterns suggesting NiO particles were also better dispersed or combined with Y_2O_3 in these catalysts. Additionally Y_2O_3 patterns were observed only for 5%Y_2O_3·Al_2O_3, which indicated that Y_2O_3 loading was higher than a monolayer for this content.

3.3. UV–vis diffuse reflectance spectroscopy (DRS)

The DRS-UV–vis spectra of the studied catalysts are shown in Fig. 2. Bands between 230 and 305 nm were observed, which indicate the presence of free NiO [18,19]. These bands were not dependent on the support, indicating the presence of NiO as a precursor for all catalysts. Temperature programmed reduction experiments were then employed to further investigate these results.

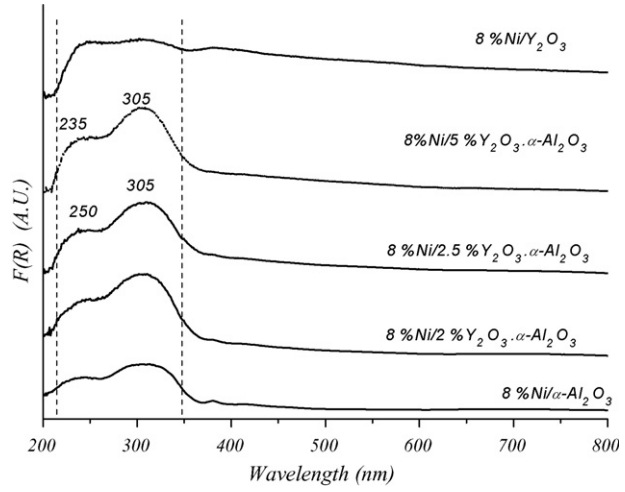

Fig. 2. DRS spectra of α-Al_2O_3, Y_2O_3 and Y_2O_3·Al_2O_3 nickel supported catalyst.

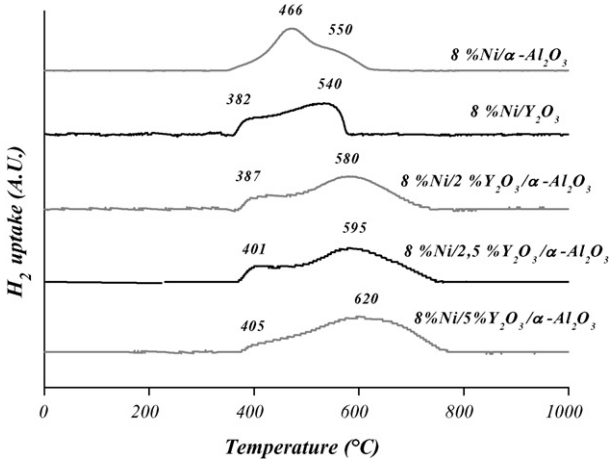

Fig. 3. Temperature programmed reduction of α-Al_2O_3, Y_2O_3 and Y_2O_3·Al_2O_3 supported nickel catalysts.

3.4. Temperature programmed reduction (TPR)

Fig. 3 shows the TPR profiles of the prepared catalysts. The profile for the 8%Ni/α-Al_2O_3 catalyst presented two main reduction peaks, at 473 °C and at 565 °C. These peaks are well described in the literature [20,21] where the first peak is attributed to NiO, which is consistent to the DRS-UV–vis results, and the second peak is due to the incorporation of Al^{3+} to NiO. During the impregnation step, there is formation of an acidic environment that causes a dissolution of Al^{3+} from the α-Al_2O_3 surface. The incorporation of these Al^{3+} ions to NiO retards the reduction of part of the NiO species, causing the appearance of the second peak in the TPR experiments. This model was fully proved by Richardson et al. [21]. For 2%Ni/α-Al_2O_3 catalysts, Pompeo et al. [22] have also observed the peaks due to NiO with different interactions with the support (at 552 and 584 °C), but they have also reported the presence of a high temperature peak at 680 °C, which was interpreted as the presence of $NiAl_2O_4$. This species was not observed in this work, due to the differences in total Ni content and pretreatment procedures. 8%Ni/Y_2O_3 catalysts presented reduction peaks at 382 and 530 °C. The first peak may be attributed to the reduction of NiO, while the second peak is related to the interaction between NiO and Y_2O_3, probably with the formation of $NiYO_3$, similarly to previously observed for Rh/Y_2O_3 [23] and for Pt/Y_2O_3 catalysts [24]. Regarding, H_2 consumption during TPR experiments, all the catalysts showed values around 1.4 mmol/g_{cat}, indicating total reduction of Ni^{2+} to Ni^0.

3.5. Hydrogen chemisorption

H_2 chemisorption measurements (Table 2) showed that all prepared catalysts presented low H/Ni ratios. However, the H/Ni values increase with yttria content, as observed by the BET areas of the support. Thus, this could be related to better nickel dispersion on supports of higher area. However, this trend was not observed in the catalytic activity results shown below, indicating this

Table 2
Irreversible H_2 chemisorption and H/Ni ratio on Ni catalysts.

Catalyst	H_2 chem. (μmol/g_{cat})	H/Ni
8%Ni/α-Al_2O_3	7.8	0.011
8%Ni/Y_2O_3	21.0	0.031
8%Ni/2%Y_2O_3·Al_2O_3	8.3	0.012
8%Ni/5%Y_2O_3·Al_2O_3	12.8	0.019
8%Ni/10%Y_2O_3·Al_2O_3	18.1	0.027

Table 3
Cyclohexane dehydrogenation at 260 °C.

Catalyst	Dehydrogenation rate ($\times 10^{-3}$ mol/h/g_{cat})	Hydrogenolysis rate ($\times 10^{-3}$ mol/h/g_{cat})
8%Ni/α-Al_2O_3	5.1	0
8%Ni/Y_2O_3	2.0	0
8%Ni/2%Y_2O_3·Al_2O_3	4.0	0
8%Ni/2.5%Y_2O_3·Al_2O_3	4.4	0
8%Ni/5%Y_2O_3·Al_2O_3	9.5	3.3

technique was not able to measure true nickel dispersion on these catalysts.

3.6. Cyclohexane dehydrogenation

The reaction rate of the several catalysts for the cyclohexane hydrogenation is listed in Table 3. At 260 °C the only observed product was benzene, except for the 8%Ni/5%Y_2O_3·Al_2O_3 catalysts, on which *n*-hexane, a hydrogenolysis product, was also formed. The activity increased in the following order: 8%Ni/Y_2O_3 < 8%Ni/2%Y_2O_3·Al_2O_3 ~ 8%Ni/2.5%Y_2O_3·Al_2O_3 ~ 8%Ni/α-Al_2O_3 < 8%Ni/5%Y_2O_3·Al_2O_3. This trend was different from the trend observed for H_2 chemisorption, but the activity for the autothermal of methane followed this same order as shown below.

3.7. Autothemal reforming of methane

The results for autothermal reforming of methane are displayed in Figs. 4–7 and in Table 4. The 8%Ni/α-Al_2O_3 catalyst presented an initial conversion equal to 65%, but it deactivated during 24 h time-on-stream to a final conversion of 18%. The 8%Ni/Y_2O_3 catalyst was quite stable within 24 h time-on-stream, but it displayed a low conversion (around 20%). The low activity for this catalyst in the autothermal reforming of methane was consistent with the cyclohexane dehydrogenation results, for which the 8%Ni/Y_2O_3 catalyst also presented a low activity, but it was not proportional to hydrogen chemisorption results, indicating this technique was not adequate for measuring catalytic sites for this catalyst.

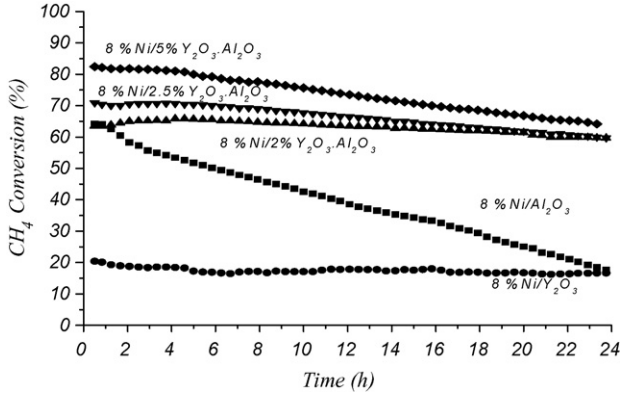

Fig. 4. Autothermal reforming of methane on α-Al_2O_3, Y_2O_3 and Y_2O_3/Al_2O_3 nickel supported catalysts (T = 800 °C, CH_4:O_2:H_2O = 2:1:0.4).

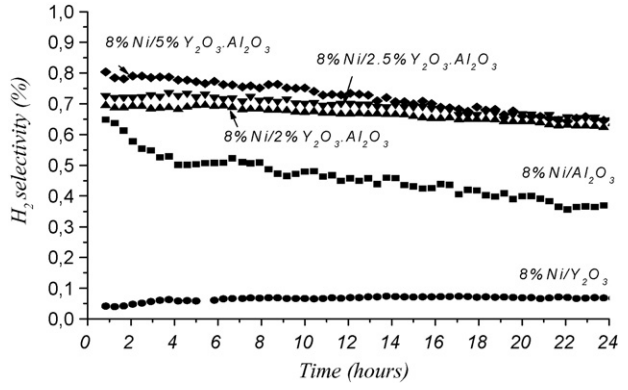

Fig. 5. H_2 selectivity in autothermal reforming of methane on α-Al_2O_3, Y_2O_3 and Y_2O_3/Al_2O_3 nickel supported catalysts (T = 800 °C, CH_4:O_2:H_2O = 2:1:0.4).

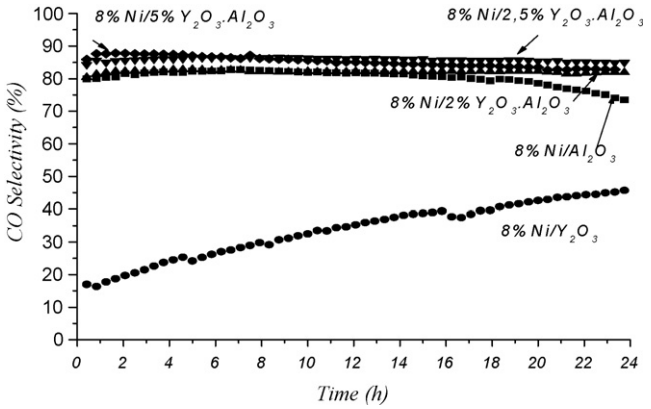

Fig. 6. CO selectivity in autothermal reforming of methane on α-Al_2O_3, Y_2O_3 and Y_2O_3/Al_2O_3 nickel supported catalysts (T = 800 °C, CH_4:O_2:H_2O = 2:1:0.4).

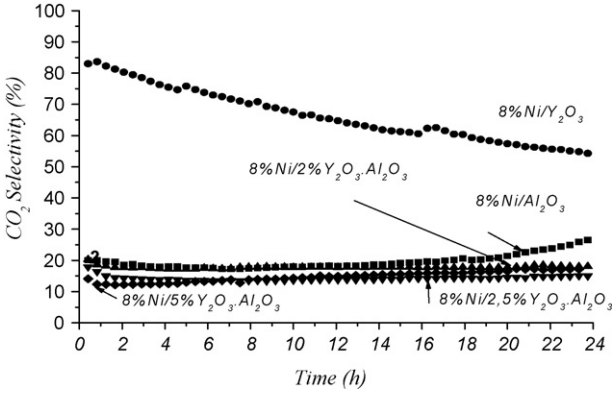

Fig. 7. CO_2 selectivity in autothermal reforming of methane on α-Al_2O_3, Y_2O_3 and Y_2O_3/Al_2O_3 nickel supported catalysts (T = 800 °C, CH_4:O_2:H_2O = 2:1:0.4).

The Y_2O_3/Al_2O_3 supported catalysts presented higher initial methane conversions (Fig. 4 and Table 4), with the increase of yttria content, and also the stability was improved with the addition of yttria to Ni/α-Al_2O_3. In general, initial methane conversions followed the same trend as cyclohexane dehydrogenation reaction rates. This way, the use of this model reaction, which is structure insensitive, provided better estimates of the number of surface active sites than hydrogen chemisorption for these catalysts. This behavior was also observed for Pt/CeO_2·ZrO_2 investigated in the partial oxidation of methane [24], and may be related to the effect of the support on the metal active sites.

The initial selectivities for H_2 and CO (Figs. 5 and 6) followed the same trend as the initial conversion of methane, i.e., the more active catalysts presented higher H_2 and CO selectivities. Additionally, the H_2 and CO selectivities decreased with time due to the deactivation of the catalysts. CO_2 selectivities, on the other hand, showed opposite behavior. These results are consistent with the so-called indirect mechanism usually applied for the partial oxidation of methane. In the first step, there is combustion of methane, producing CO_2 and H_2O and in the second step H_2O and CO_2 reforming of unreacted methane take place, forming H_2 and CO [24,25]. This way, when the catalyst deactivates, there is an

Table 4
CH_4 conversion and H_2/CO ratio.

Catalyst	CH_4 conversion (%)		H_2/CO	
	Initial	Final[a]	Initial	Final[a]
8%Ni/α-Al_2O_3	65.0	17.6	1.4	1.2
8%Ni/Y_2O_3	21.1	17.1	1.4	1.3
8%Ni/2%Y_2O_3·Al_2O_3	63.0	58.7	1.6	1.7
8%Ni/2.5%Y_2O_3·Al_2O_3	70.9	59.8	2.0	1.8
8%Ni/5%Y_2O_3·Al_2O_3	82.4	64.2	2.0	1.7

[a] After 24 h time-on-stream.

inhibition of the second step of CO_2 reforming, causing a decrease in H_2 and CO selectivity and an increase in CO_2 selectivity as observed for the results presented in this work. The H_2/CO ratios for the several catalysts (Table 6) were also related to the deactivation of the catalysts, as these values decreased for the Ni/Al_2O_3 catalysts which showed considerable deactivation. Initial H_2/CO values were around 2 for the catalysts supported on Y_2O_3·Al_2O_3, which presented higher activity, and the values were kept constant time-on-stream, as these catalysts have not shown deactivation.

3.8. Temperature programmed oxidation (TPO)

TPO profiles of spent catalysts are presented in Fig. 8, while the amount of CO_2 released during TPO experiments is shown in Table 5. The TPO profile of 8%Ni/α-Al_2O_3 displayed three peaks. The first one at 410 °C may be attributed to monoatomic carbon species on Ni atoms (type I) [26,27], the peak at 480 °C (type II) is ascribed to filamentous coke and the peak at 580 °C (type III) may be attributed to the formation of graphitic coke [15,20,23,28].

For the Y_2O_3 containing catalysts, additional peaks were formed at higher temperatures (700–800 °C), indicating the formation of either a new type of coke or coke located in different positions. Although, we do not have enough information to fully characterize this high temperature peak, the results indicate that it is related to the higher stability observed for the Y_2O_3 containing catalysts. The amount of coke formed for the several catalysts was about the same (Table 5), indicating that in the case of the Y_2O_3 containing

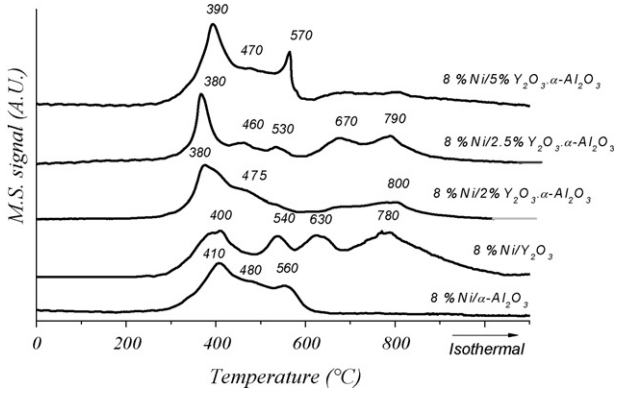

Fig. 8. TPO profiles of α-Al_2O_3, Y_2O_3 and Y_2O_3/Al_2O_3 nickel supported catalysts used on autothermal reforming of methane.

Table 5
Amount of CO_2 formed during TPO experiments on spent Ni catalysts.

Catalyst	Amount of formed CO_2 (mmol/g_{cat})
8%Ni/Al_2O_3	1.2
8%Ni/Y_2O_3	0.9
8%Ni/2%Y_2O_3·Al_2O_3	1.0
8%Ni/2.5%Y_2O_3·Al_2O_3	1.1
8%Ni/5%Y_2O_3·Al_2O_3	1.2

Table 6
Cyclohexane dehydrogenation activity for fresh and aged Ni catalysts (T = 260 °C).

Catalyst	Fresh (mmol/g_{cat})	Aged (mmol/g_{cat})
8%Ni/α-Al_2O_3	5.1	5.0
8%Ni/Y_2O_3	2.0	2.2
8%Ni/2%Y_2O_3·Al_2O_3	4.0	4.4
8%Ni/2.5%Y_2O_3·Al_2O_3	4.4	5.0
8%Ni/5%Y_2O_3·Al_2O_3	9.5	10.8

catalysts, nickel species were not covered by this new type of coke. One possibility is an ensemble effect on Ni particles with the presence of Y_2O_3 [1,20]. Another possibility is to follow the Ruckenstein and Wang [23] suggestion for Rh/Y_2O_3 catalysts of a formation of a quasi-steady-state concentration of metallic sites due to the moderation of the oxidation and reduction rates of the metal particles, which would keep metallic nickel available to the reaction, due to the formation of a $NiYO_3$ compound.

3.9. Catalyst ageing experiments

In order to verify whether, under the reaction conditions used, the catalysts were submitted to deactivation by sintering besides coke deposition, an ageing procedure was envisaged to simulate the reaction conditions, as described in Section 2. Table 6 lists the rates for cyclohexane dehydrogenation of the catalysts aged at the same temperature, steam partial pressure and time used in the autothermal reforming of methane, and the rates observed for the fresh catalysts. The reaction rates were very similar for fresh and aged catalysts, showing that sintering was not relevant under the autothermal reforming reaction conditions tested in this work. This way, the observed differences after adding Y_2O_3 to Ni/α-Al_2O_3 may be explained by a change in the coke formation mechanism.

4. Conclusions

The effect of Y_2O_3 addition to Ni/α-Al_2O_3 catalyst was investigated in the autothermal reforming of methane. There was an increase in the activity and in the stability of the catalysts for this reaction. This behavior was explained by the formation of an intermediate surface compound between Ni and Y_2O_3 which provided a protection of the nickel particles from carbon deposition.

Acknowledgements

The authors are grateful for the financial support received from CAPES and from PETROBRAS (GTL program).

References

[1] J.R. Rostrup-Nielsen, J. Sehested, Adv. Catal. 47 (2002) 65.
[2] K. Aasberg-Petersen, T.S. Christensen, C.S. Nielsen, I. Dybkjær, Fuel Process. Technol. 83 (2003) 253.
[3] D.J. Wilhelm, D.R. Simberck, A.D. Karp, R.L. Dickenson, Fuel Process. Technol. 71 (2001) 139.
[4] J.N. Armor, Appl. Catal. A: Gen. 176 (1999) 159.
[5] M.A. Peña, J.P. Gómez, J.L.G. Fierro, Appl. Catal. A: Gen. 144 (1996) 7.
[6] S. Ayabe, H. Omoto, T. Utaka, R. Kikuchi, K. Sasaki, Y. Teraoka, K. Eguchi, Appl. Catal. A: Gen. 241 (2003) 261.
[7] A. Parmaliana, F. Arena, F. Frusteri, S. Coluccia, L. Marchese, G. Martra, A.L. Chuvilin, J. Catal. 141 (1993) 34.
[8] Y.H. Hu, E. Ruckenstein, Adv. Catal. 48 (2004) 297.
[9] G.B. Sun, K. Hidajat, X.S. Wu, S. Kawi, Appl. Catal. B: Environ. 81 (2008) 303.
[10] F. Pompeo, N.N. Nichio, O.A. Ferreti, D. Resasco, Int. J. Hydrogen Energy 30 (2005) 1399.
[11] H-a. Nishimoto, K. Nakagawa, N.-O. Ikenaga, T. Suzuki, Catal. Lett. 82 (2002) 161.
[12] C. Karunakaran, R. Dhanalakshmi, P. Anilkumar, Radiat. Phys. Chem. 78 (2009) 173.
[13] H.Y. Wang, E. Ruckenstein, Appl. Catal. A: Gen. 204 (2000) 143.

[14] A.G. Gaikwad, S.D. Sansare, V.R. Choudhary, J. Mol. Catal. A: Chem. 181 (2002) 143.
[15] S. Wang, G.Q.M. Lu, Appl. Catal. B: Environ. 16 (1998) 269.
[16] T. Zhu, M.F. Stephanopoulos, Appl. Catal. A: Gen. 208 (2001) 403.
[17] J. Sun, X. Qiu, F. Wu, W. Zhu, J. Wang, Int. J. Hydrogen Energy 30 (2005) 437.
[18] E. Kis, R. Marinkovíc-Neducin, G. Lomic, G. Boskovic, D.Z. Obadovic, J. Kiurski, P. Putanov, Polyhedron 17 (1998) 27.
[19] F. Delannay, Characterization of Heterogeneous Catalysts, Marcel Dekker, New York, 1984.
[20] J.S. Lisboa, D.C.R.M. Santos, F.B. Passos, F.B. Noronha, Catal. Today 101 (2005) 15.
[21] J.T. Richardson, M. Lei, B. Turk, K. Foster, M.V. Twigg, Appl. Catal. A: Gen. 110 (1994) 217.
[22] F. Pompeo, N.N. Nicchio, M.M.V.M. Souza, D.V. Cesar, O.A. Ferretti, M. Schmal, Appl. Catal. A: Gen. 316 (2007) 175.
[23] E. Ruckenstein, H.Y. Wang, J. Catal. 190 (2000) 32.
[24] F.B. Passos, E.R. Oliveira, L.V. Mattos, F.B. Noronha, Catal. Lett. 110 (2006) 161.
[25] M. Prette, C. Eichner, M. Perrin, Trans. Faraday Soc. 43 (1946) 335.
[26] D. Duprez, K. Fadili, J. Barbier, Ind. Eng. Chem. Res. 36 (1997) 3180.
[27] L. Zhang, X. Wang, B. Tan, U. Ozkan, J. Mol. Catal. A: Chem. 297 (2009) 26.
[28] H.M. Swaan, V.C.M. Kroll, G.A. Martin, C. Mirodatos, Catal. Today 21 (1994) 571.